Experimental study on the role of chromatic dispersion in continuous-wave supercontinuum generation

L. Abrardi[1], **S. Martin-Lopez**[1], **A. Carrasco-Sanz**[1], **F. Rodriguez-Barrios**[1], **P. Corredera**[1], **M. L. Hernanz**[1]
1. *Instituto de Fisica Aplicada, Consejo Superior de Investigaciones Cientificas (CSIC)*
C/ Serrano 144, 28006 Madrid, Spain
M. Gonzalez-Herraez[2]
2. *Departamento de Electronica, Universidad de Alcala. Edificio Politecnico, Campus Universitario*
28871 Alcala de Henares, Madrid, Spain

The influence of chromatic dispersion on CW-pumped supercontinuum generation in km-long standard fibers is experimentally investigated. We perform our study by means of a tunable, high-power fiber ring laser pumping a dispersion-shifted fiber in the wavelength range of small and medium anomalous dispersion. Our results show that, at low input powers, chromatic dispersion plays a dominant role on nonlinear pump spectral broadening, giving rise to a broader spectrum when pumping just above the zero-dispersion wavelength of the fiber. At higher input powers, however, the width of the generated supercontinuum spectrum is mostly due to the Raman effect, hence more independent of the value of the chromatic dispersion coefficient. We show that, in this case, the optimum pumping wavelengths for supercontinuum generation are not so close to the zero-dispersion wavelength of the fiber as in the previous case. In these conditions, as the chromatic dispersion grows we can obtain square-shaped and high-power density spectra, which seem extremely promising for applications in optical coherence tomography.

Keywords: nonlinear optics, supercontinuum, chromatic dispersion, dispersive waves, soliton self-frequency shift

I. INTRODUCTION

Nowadays, fiber-based supercontinuum (SC) sources find widespread applications in many different fields, including telecommunications, spectroscopy and medical imaging techniques like optical coherence tomography [1], [2]. In particular, continuous-wave (CW) SC generation in optical fibers has attracted much attention in the last years for the possibility of developing compact, high-quality sources for ultrahigh resolution optical coherence tomography. Among their good properties, these sources exhibit extremely short coherence lengths (allowing resolutions of only several micrometers), high power spectral densities (normally in the order of several mW/nm) and lower values of relative intensity noise (RIN) than their pulsed counterparts [3], [4].

The process of converting a CW laser emission into supercontinuum in optical fibers has been studied intensively in the last years, both experimentally [5], [6], [7], [8], [9], [10] and theoretically [11], [12], [13], [14]. These studies have shown that CW SC sources are initiated by modulation instability (MI) of the partially coherent input beam, **which can lead to soliton formation and collision processes [15], [14]**. Then, the Raman scattering induces a self-frequency downshift of the generated solitons, so that their final spectral distribution covers a wide wavelength range. The creation of a soliton is accompanied by the generation of a dispersive wave frequency up shifting as the soliton down shifts because of the Raman scattering. Although the dynamics of CW SC generation are reasonably understood nowadays, many efforts are still being done in order to improve and optimize the supercontinuum properties, such as higher spectral power density, larger spectral width, smoother spectral profile and better long-term stability. As an example, in a previous paper [16] we studied the influence of pump incoherence in CW SC generation. We showed experimentally, that, for a given input power and chromatic dispersion coefficient, there is an optimum value of pump incoherence that yields the most efficient spectral broadening. In this paper, we use a similar methodology to study the dependence of CW SC generation on chromatic dispersion. This study seeks to understand possible strategies to optimize the fiber dispersion so as to improve the SC properties.

Chromatic dispersion plays a key role in the processes of modulation instability and soliton **formation**. The most obvious limit is that these processes efficiently occur in the anomalous dispersion region of the fiber. **Besides, at smaller anomalous dispersion values the MI oscillations are temporally faster and induce shorter pulse formation [17]. This effect leads to the generation of shorter solitons which undergo a larger red-shift per fiber length due to intrapulse Raman scattering [18], [19].** Soliton compression can also be induced by use of dispersion management [9], [10], [20], leading to enhanced supercontinuum spectra.

In this work we present an exhaustive experimental study of the influence of chromatic dispersion on supercontinuum

spectral broadening generated with continuous wave light in a standard dispersion-shifted fiber (DSF). This is done by tuning the wavelength of the high-power pump laser over the spectral region of small and moderate anomalous chromatic dispersion of the fiber. This paper shows that beyond a certain power level there is a range of chromatic dispersion values for which the spectral width of the supercontinuum remains constant. This range of values is broader as the pump power increases. Additionally, we show that the optimum shape of the SC is actually obtained for moderate values of chromatic dispersion. These results are, in our view, very interesting from a practical and engineering point of view, and we explain them qualitatively based on the established explanation of CW SC generation.

This paper is organized as follows: in the following section, the experimental setup is described. In Section III we discuss the effect of chromatic dispersion on soliton dynamics and dispersive wave generation; in section IV we show experimental results on the dependence of supercontinuum spectral width on chromatic dispersion. Experimental results show that broadband SC can be efficiently generated by CW pumping over a wide range of dispersion values when using km-long standard fiber at input powers of several watts. Finally, in Section V we derive the conclusions of our study.

II. EXPERIMENTAL SET-UP

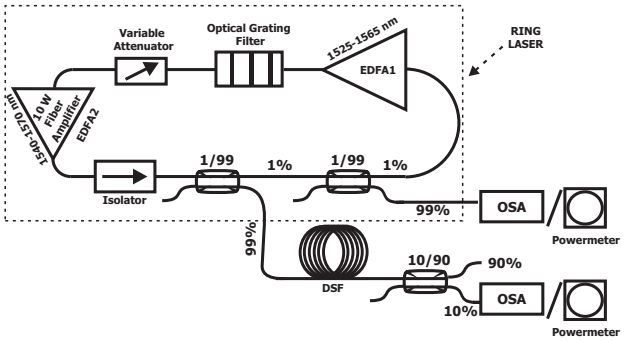

Fig. 1. Experimental setup. EDFA: Erbium-Doped-Fiber amplifier; DSF: Dispersion Shifted Fiber; OSA: Optical Spectrum Analyzer.

In order to make an experimental study on the influence of chromatic dispersion on nonlinear spectral broadening, we need to have the way to pump the fiber at different dispersion values, or equivalently, at different wavelengths. The wavelength range that we treat here is such that the nonlinear coefficient, Raman gain and losses of the fiber do not vary too much, but the dispersion does vary significantly. The pumping is realized by means of a home-made high-power tunable laser source. Our pump is a fiber ring laser mainly made up of two Erbium doped fiber amplifiers (EDFAs) and a tunable optical grating filter, as shown in Fig. 1. EDFA1 (EDFA-C17 provided by NetTest) has gain in the wavelength range of 1525-1570 nm and its pumping power is settled to slightly over transparency. After EDFA1, an optical grating filter is inserted (TB9 provided by JDS Uniphase) which is used to select the desired frequency out of the EDFA1 emission. It provides a tuning range of 1525-1625 nm and a spectral width of 0.5 nm full width at half a maximum (FWHM). The grating filter is followed by a variable attenuator (provided by Accelink) which is used to control the power inserted into EDFA2. In fact, we want to guarantee that EDFA2 is working at the same saturation level at all wavelengths. EDFA2 is a high-power fiber amplifier (Keopsys) working in the spectral range 1545-1570 nm, whose output power can take values from 200 mW to 10 W. A high-power isolator (OPNETI) is inserted at the output of EDFA2 to prevent damage in the amplifier by back-reflected light and backward Raman. The isolator losses are approximately 0.5 dB. Only 0.01% of the power delivered by EDFA2 is re-circulated in the cavity. This is done by means of a set of two calibrated 1/99 couplers. We used the remaining port to monitor the output power of the fiber laser. This arrangement allows us to generate a tunable source whose output power takes the same value for each wavelength during our measurements. The described fiber ring laser is single-mode, it presents a 0.08 nm FWHM line width at every wavelength in the available tuning range (i.e. from 1545 nm to 1570 nm) and its power can take values from 500 mW to 7 W. The laser output can be seen in Fig. 2 at different wavelengths for a total output power of 2 W.

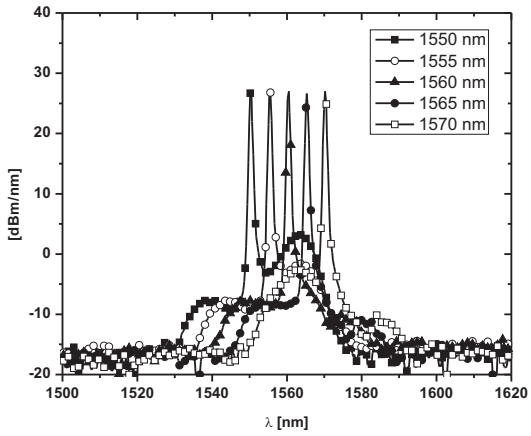

Fig. 2. Laser output at different wavelengths. The total output power is 2 W.

The fiber is a 11 km DSF provided by Corning. The dispersion curve of the fiber has been measured using the phase-shift method described in [21] with a resolution of 2 nm. Both λ_{ZD} and the nonlinear coefficient γ have been measured with an alternative scheme using a method based on modulation instability [22], [23], [24] and found to take values λ_{ZD} = 1553.5±0.5 nm, and γ = 1.7 $\mathrm{W^{-1}km^{-1}}$. In the tuning range of our ring-cavity laser the group-velocity dispersion (GVD) parameter β_2 is linearly decreasing with a slope of -0.1044 $\mathrm{ps^2/km/nm}$ and it takes value 0.7828 $\mathrm{ps^2/km}$ at λ = 1545 nm and -1.8266 $\mathrm{ps^2/km}$ at λ = 1570 nm. The third and fourth-order-dispersion parameters (TOD and FOD respectively) can be considered almost constant over the whole tuning range, and they take values β_3 = 0.1358 ± 0.00377 $\mathrm{ps^3/km}$ and β_4 = -4.8739 × 10^{-4} ± 0.0560 × 10^{-4}

$\mathrm{ps}^4/\mathrm{km}$ respectively. Since higher order dispersion parameters are almost constant, we can make a study of the influence of second-order dispersion parameter on spectral broadening and neglect the influence of higher order dispersion terms. The output spectrum is finally analyzed by means of an optical spectrum analyzer (OSA) with a spectral resolution of 1 nm after passing through a 10/90 coupler, which acts uniquely as fixed attenuator. The input and output power are measured by means of an integrating sphere radiometer whose responsivity is known in the whole tuning range with 1% uncertainty [25].

III. ANOMALOUS DISPERSION REGIME AND DISPERSIVE WAVE GENERATION

This work seeks to give a deeper insight into the effect of chromatic dispersion on supercontinuum generation in km-long conventional fibers. CW-pumped spectral broadening in fibers results from the fission of the partially coherent input CW beam into a sequence of Raman-shifted solitons through the combined effects of modulation instability and Stimulated Raman Scattering (SRS). CW-induced spectral broadening is initiated by modulation instability which breaks-up the CW radiation into a train of ultrashort pulses when propagating in the wavelength region of anomalous dispersion of the fiber. As the pulses propagate, the MI-generated pulses are split into fundamental first order solitons (one-soliton) [12] which undergo a spectral shift towards longer wavelengths due to SRS. This process of Soliton Self Frequency Shift (SSFS) gives rise to a smooth and wide spectrum lying at wavelengths longer than the pump wavelength. Additionally, each fundamental soliton can, in the presence of higher-order dispersion, release excess energy in the form of dispersive waves, enhancing the spectral broadening **in the normal dispersion region of the fiber [26]**. **These linear waves are emitted only when the soliton spectrum overlaps with the resonant wave frequencies. The amplitude of the DW radiation is proportional to the amplitude of the soliton at the phase-matched frequencies [26], so that more intense radiation is released by solitons that are closer to λ_{ZD}.**

The most obvious impact of chromatic dispersion on soliton dynamics appears through MI. In fact, CW-light propagating in the anomalous dispersion regime of an optical fiber breaks-up into a train of **solitonlike pulses** due to MI. **As the MI oscillation frequency is inversely proportional to $\sqrt{\beta_2}$ [27], shorter solitons are expected to be generated when pumping closer to λ_{ZD} [17], [28]. As shorter solitons red-shift faster due to SSFS [18], [19], a much wider spectrum is expected to be generated when pumping closer to λ_{ZD}.** Thus, it is clear that under no other effects, the most efficient nonlinear broadening **is expected at** GVD parameters as close to zero as possible. However, in the next section we will see that beyond a certain input power, Raman scattering becomes the dominant nonlinear effect in these km-long fibers. In this case, soliton self-frequency shift is the dominant broadening mechanism, and the importance of chromatic dispersion is radically smaller.

We now look at the blue-shifted part of the SC spectrum. **Dispersive waves are not only radiated by fundamental solitons in the presence of higher order dispersion perturbation. If sufficiently high power is injected into the fiber in anomalous dispersion regime, a train of N-solitons can be generated. In this case,** dispersive waves arise from higher-order soliton, which are unstable under higher-order dispersion and decay into fundamental solitons. **These latter ones eject excess of energy as dispersive radiation in the normal dispersion region of the fiber [29], [30], [31], [32], [33].**

Previous theoretical and experimental studies [30], [26], [34] show that dispersive waves are generated when the soliton spectrum overlaps the resonance frequency which fulfills the following phase matching condition:

$$\beta(\omega_{DW}) - \beta(\omega_S) = \sum_{n\geq 2}^{M} \frac{\beta_n}{n!}\delta\omega^n + \frac{\gamma\ P_S}{2} = 0 \qquad (1)$$

where $\beta(\omega_{DW})$ is the wave **number** of the dispersive radiation, $\beta(\omega_S)$ is the wave **number** of the soliton, $\delta\omega = (\omega_{DW} - \omega_S)$ is the detuning between the radiation frequency ω_{DW} and the central soliton frequency ω_S and β_n is the n-th derivative of $\beta(\omega)$ calculated at ω_S; $\gamma \mathrm{P_S}/2$ is the soliton nonlinear phase shift, γ is the nonlinear **parameter of the fiber [27]** and $\mathrm{P_S}$ is the soliton peak power. This equation allows to predict the dispersive wave frequency once the dispersion parameters of the fiber **and the soliton carrier frequency** are known. The resonant radiation frequency depends weakly on the soliton amplitude [26], [35], so that the nonlinear phase-shift term can be often neglected in Eq. 1. In this case, the phase matching condition is equivalent to:

$$\sum_{n\geq 2}^{M} \frac{\beta_n}{n!}\delta\omega^{n-2} = 0 \qquad (2)$$

where the two degenerate solutions $\delta\omega = 0$ ($\omega_{DW} = \omega_S$) have been obviously discarded. In our experiment we

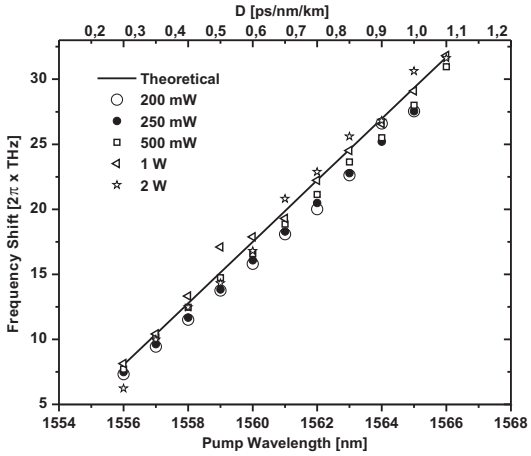

Fig. 3. DW-frequency shift as function of pump wavelength for different input powers

observed that the blue-part of the spectrum shows a maximum in intensity that, for a given input wavelength, always falls at the same frequency for different input powers. As we can not measure the central frequency of the generated solitons, we make the hypothesis that most of the DWs are radiated at the first stage of soliton formation, when solitons are expected to have central wavelength just above the pump wavelength. According to this hypothesis, we calculated the DW frequency that would be radiated by a soliton at the pump frequency by substituting $\omega_S = \omega_P$ in Eq.2 using the series expansion until the fourth order (M=4). We found that the frequency of the maximam of the blue-shifted radiation were in good agreement with this assumption. Measurements were performed at different input powers and are shown in Fig. 3 together with the theoretical curve.

As expected **from the phase-matching condition**, at higher values of dispersion **the solitons are in resonance with dispersive radiation at larger frequency shifts from the soliton carrier frequency**. **The experimental data seem to confirm that most radiation is emitted by solitons generated just above the pump wavelength, i.e. at the first stages of soliton formation, before they undergo a significant SSFS. Besides, it seems that these dynamics are not sensitive to the average injected power until a power of several watts (P=3 W in our case) is injected for which blue-shifted components are still amplified but no maxima can be seen anymore.** In Fig. 4 we show the output spectra obtained for input powers of 250 mW (a) and 1 W (b). The pump wavelength and the corresponding chromatic dispersion values are reported in the legend. Output spectra at 250 mW clearly shows MI sidebands and dispersive waves. At low pump wavelengths (1556 nm) the spectrum exhibits a typical MI asymmetric profile and intense dispersive waves, while at longer pump wavelengths (i.e. larger dispersion) the MI asymmetry is less evident and lower-intensity dispersive waves are generated.

It is worth noting that, for the same input power, the intensity of the dispersive wave decreases as the pump wavelength increases. This is consistent with the fact that the energy transfer from the soliton to the DWs depends on the spectral overlap between these two waves [26], [36]. As they become more apart with increasing pump wavelength, the overlap between them is smaller. **Besides, the spectral gap between the DW peak and the residual pump is increasing when pumping at longer wavelengths.** In Fig. 4 (b), the output spectra are shown for an input power of 1W. At this input power, MI sidebands can not be appreciated anymore and large spectral broadening and strong pump depletion start to take place. **Dispersive waves present higher intensity then the previous case.** This is clearly visible in Fig. 4 (b). **We also show that, as expected, for a too large detuning between the pump and λ_{ZD}, the soliton spectrum does not overlap with the phase-matched frequencies and DW amplification can not take place,** which is the case for example when pumping at 1570 nm. This process, **which is consistent with previous results in microstructured fibers [30], [32]**, is made clearer by a 3D representation of our spectra. In Fig. 5 the output spectrum evolution is shown as function of pump wavelength for an input power of 1W. There is a clear sign of dispersive waves, and the transition from normal to anomalous dispersion around 1554 nm is also evident by a large spreading of the output spectrum. We note that the dependence of MI and

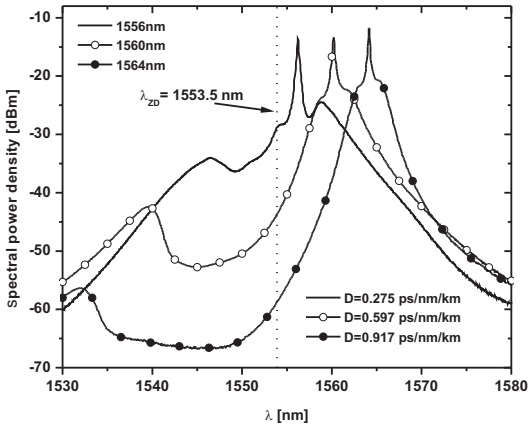

(a)

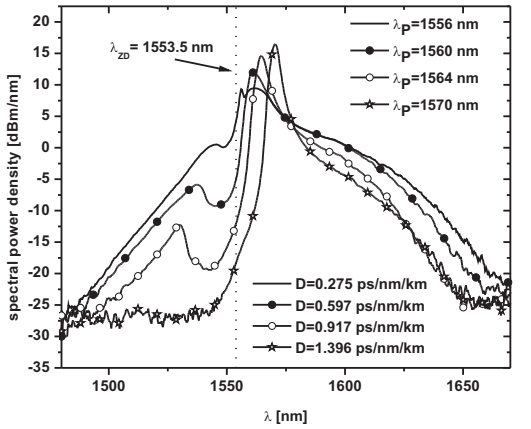

(b)

Fig. 4. Modulation instability and dispersive wave generation in different dispersion regimes. (a): Spectra are shown for an input power of 250 mw; (b) spectra are shown for an input power of 1 W.

dispersive waves on chromatic dispersion gives rise to SC spectra having a completely different shape for different pump wavelengths and powers. In particular, at this value of input power the spectrum is flatter and broader when the pump wavelength is just above the zero-dispersion wavelength of the fiber λ_{ZD} = 1553.5 nm. **In Fig. 7 the ratio between the maximum DW intensity and the residual pump intensity is plotted for different average input powers. It is interesting to observe that this ratio grows with increasing input power below P=1W. When higher powers are injected into the fiber, this ratio remains almost constant. Moreover, when the pump power is higher than 1 W, dispersive**

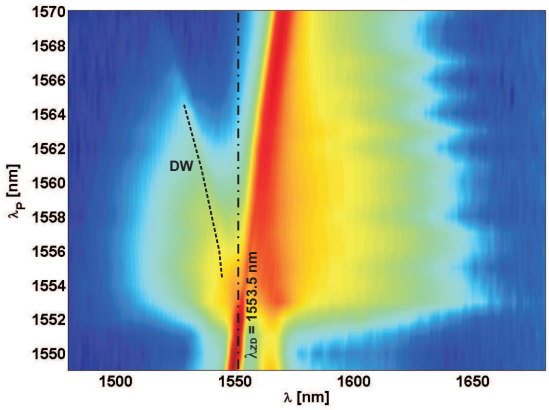

Fig. 5. Output spectra as function of pump wavelength λ_P (vertical axis) for an input power of 1W. We can see that DWs give a significant contribution to spectral broadening only when pumping just above λ_{ZD}. For increasing pumping wavelength, their intensity is decreasing and the spectral gap between the residual pump and the DW peak is increasing. For $\lambda_{\rm P}$ >1566 nm there is no DW amplification and the whole SC spectrum lies at wavelengths longer than λ_{ZD}.

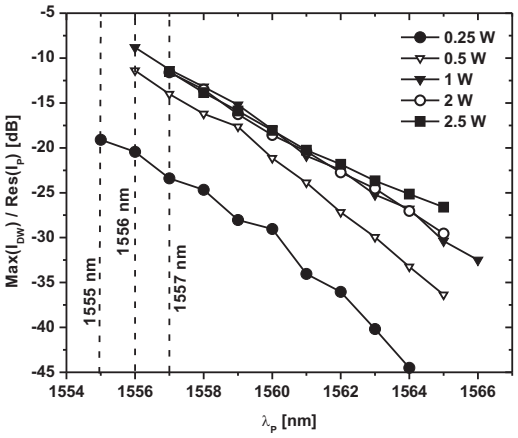

Fig. 7. Ratio between the DW peak intensity and the residual pump intensity.

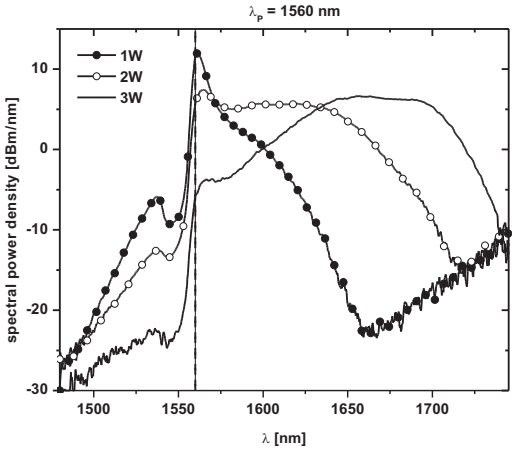

Fig. 6. Supercontinuum spectra obtained at three different input powers. The pump wavelength is λ_P=1560 nm and marked with a dashed line in the picture.

waves start to undergo attenuation with increasing input power, as it can be seen in Fig. 6. In this case, however, flatter supercontinua are obtained for longer wavelengths (i.e. larger values of dispersion), as we will see in the next section. Since the Raman threshold in our case is estimated to be $\mathrm{P_{cr}} \sim 1\mathrm{W}$ [27] by taking the Raman gain coefficient $\mathrm{g_R}$=1.5$\times 10^{-11}\mathrm{cm/W}$ for silica fibers [37], we believe that these results are the clear signature of the increasing role of Raman scattering on SC dynamics in this km-long silica fiber. It is now important to point out that the presence of a well defined peak in the blue part of the spectrum seems to indicate that higher-order solitons are not generated or, eventually, only low order solitons are formed (N$\sim$1). In fact, if the dispersive radiation were the result of soliton fission dynamics, a much broader and flatter blue-shifted spectrum would be generated due to the contribution of the N-soliton decay into N fundamental solitons of different central frequency [29], [30]. Besides, when DWs are radiated by fundamental solitons from higher-order soliton fission, a maximum of intensity should appear at the blue edge of the spectrum [30], [32], which is not our case. Instead, our results are consistent with theoretical predictions for which in CW-pumping regimes fundamental solitons of slightly different amplitude and time duration originate from phase noise of the pump due to MI [11], [12], [14]. Immediately after formation they release non-solitonic radiation in the presence of higher-order dispersion and continue to radiate some energy while Raman red-shifting until stability is reached. On the other side, some authors also proved that MI-induced solitons have too long time duration to undergo a significant SSFS [38] and generate broad supercontinua. Some new effect other than soliton fission have to be taken into account. For this reason, our results seem to be in very good agreement with the latest theoretical studies that attribute to soliton collisions a significant role in enhancing the spectral width by leading to shorter soliton formation [14]. Moreover, new results have been published that reveal the influence of statistical processes on enhanced spectral broadening because of the generation of rare extremely red-shifted solitons [39], [40]. In particular, our experimental conditions correspond to the theoretical model presented by Dudley et Al. [40] where they point out the role of pump noise as well as of the interplay between MI and Raman scattering on rogue soliton generation, that leads to further spectral broadening at longer wavelengths.

IV. INFLUENCE OF CHROMATIC DISPERSION ON SC SPECTRAL BROADENING

In this section we analyze experimentally how chromatic dispersion affects SC spectral broadening in high-power regimes when propagating a CW radiation into a km-long conventional DSF. As we have already mentioned, our high-power tunable CW laser allows us to pump at different dispersion values of the fiber. Now we can study how chromatic dispersion influences the properties of SC spectra at different values of the total injected power. As it has been already pointed out in **a** recent SC review [34], these results are of very practical interest because there is a lack of experimental studies in the field of CW SC generation due to the limited high-power **CW** sources available. **In this section** we want to analyze the SC spectral width. As we have already mentioned, SC spectra exhibit very different shapes when pumping at different wavelengths (see Fig. 4 (b)). In order to compare the mentioned spectra among each other, we need to introduce a clear definition of SC spectral width which takes into account their different shape and their different spectral power density distribution. So far SC spectral width has been usually defined in logarithmic scale as the width measured 20-dB down from the highest peak of the spectrum. This definition hardly takes into account the effective available spectral width when the spectrum takes an asymmetric and complicated shape or a significant gap between its longer-wavelength part and its blue-shifted part. This situation makes difficult to compare spectral widths obtained for the same input power but at different pump wavelengths by using the common definition of spectral width. In order to overcome this problem we decided to use another definition of spectral width according to the standards we found in literature. In ultrashort pulse measurements, a definition of Equivalent Pulse Width (EPW) is used when the pulse shape is quite complicated (see [41]). Following this idea, we adopted the definition of Equivalent Spectral Width (ESW) to assign a spectral width value to each of our spectra with a consistent and unique method. We define the ESW of a SC source as:

$$w_e = \frac{2}{I_{max}} \int_{-\infty}^{\infty} I(\lambda) d\lambda \qquad (3)$$

where w_e is the ESW, I(λ) is the spectral power density in mW/nm, and $I_{\max}$ is the **maximum power density** of the spectrum in mW/nm. An illustration of the definition of ESW can be seen in Fig. 8. It is worth noticing that this definition uses the total power under the spectral curve, so that all the generated spectral components are taken into account. Moreover, a higher value of ESW is assigned to flatter spectra because the maximum peak is usually lower. For example when full depletion occurs, the maximum spectral power density usually takes a lower value, generating a higher value of ESW. This definition is very useful when spectral widths of different supercontinua have to be compared. In fact it favors wider and flatter profiles because it assigns them a higher ESW value. By using the definition of ESW we want to study the influence of chromatic dispersion on SC spectral broadening. With the help of our tunable source we can pump in the spectral range from 1549 nm to 1570 nm, where the chromatic dispersion of the fiber takes values from -0.291 ps/nm/km to +1.396 ps/nm/km. Within this spectral range, all the rest of the higher-order dispersion terms, the nonlinear coefficient and the attenuation of the fiber remain reasonably constant.

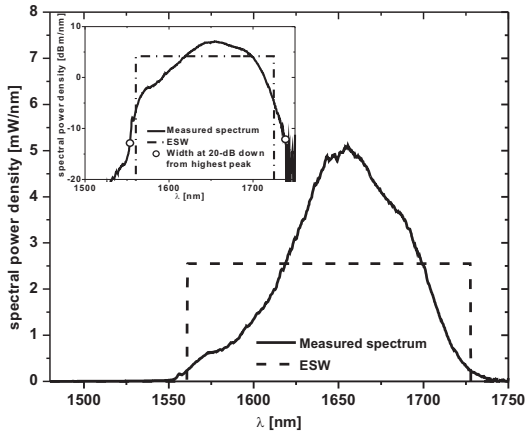

Fig. 8. Equivalent Spectral Width. The peak of the equivalent spectrum is equal to half the peak of the real spectrum. The width of the equivalent spectrum is such that its area is equal to that of the real one. The equivalent spectrum is centered at such a wavelength so as to have the minimum mean square error between the real spectrum and the equivalent one. The calculated ESW is compared with the standard measurement 20-dB down from the highest peak in logarithmic scale

The ESW as function of pump wavelength is shown in Fig. 9 for different input powers. As it can be seen, **for input powers up to the Raman threshold (P∼1 W)**, there is an optimum pump wavelength for which the ESW is maximum. This demonstrates that, in this range of powers, the optimal

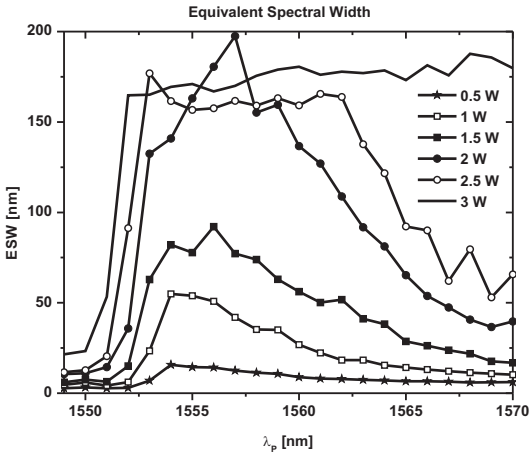

Fig. 9. Supercontinuum spectral broadening at different input powers as function of pump wavelength

pump wavelength to generate a SC source falls just above the λ_{ZD} of the fiber, which is in good agreement with the discussion of section III. At an input power of 0.5 W and 1 W, this maximum corresponds to the pump wavelength of 1554 nm, which is just above the λ_{ZD} of the fiber. In fact,the output spectra show a quite different shape and width when pumping at different wavelengths with a total power, as we have seen in Fig. 4 (b). The closer to the λ_{ZD} the laser wavelength is, the broader and flatter the output spectrum is, at expense of the **residual pump power**. In all cases, the transition from normal to anomalous dispersion is evident by the presence of a steep increase in the spectral broadening around the λ_{ZD} of the fiber. At higher input powers the behavior changes dramatically. At

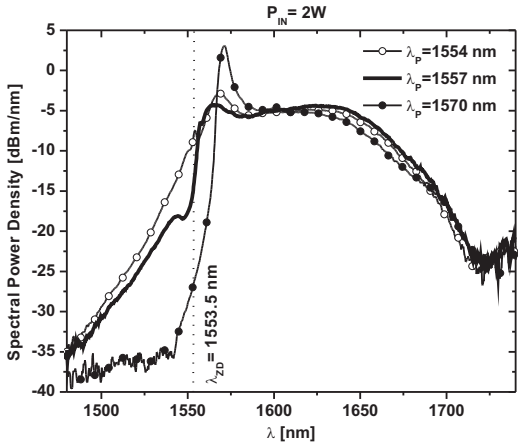

(a)

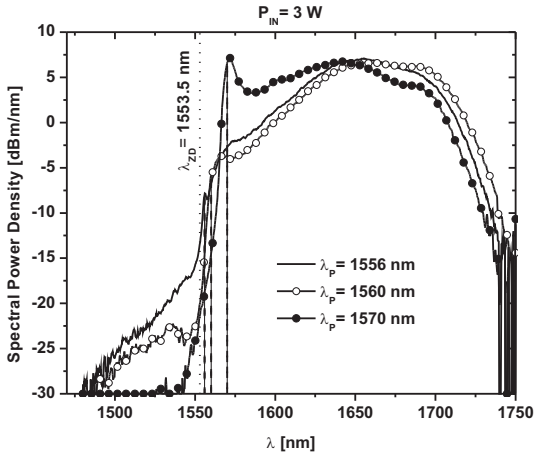

(b)

Fig. 10. Supercontinuum spectra obtained at three different pump wavelengths. (a) Output spectra obtained for an input power of 2 W. (b) Output spectra obtained for an input power of 3 W.

an input power of 2W there is an optimal pump wavelength located at 1557 nm where the ESW is maximum, but a quite wide spectral broadening can be obtained also at other pump wavelengths. **Besides, the maximum ESW at this input**

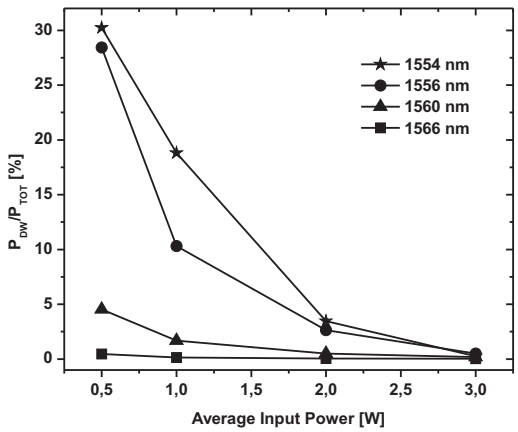

Fig. 11. Ratio between the total intensity of the spectral components in the frequency range corresponding to the anomalous dispersion region of the fiber and the total power of the whole SC spectrum. Values are shown for different pump wavelengths.

power is higher than for 2.5 W and 3 W. This is due to the fact that at this power, output spectra show a quite uniform and squared shape, and a relatively small maximum, as it can be seen in Fig.10 (a). This gives rise to a higher ESW in a consistent way with the definition of ESW which favors smoother and flatter profiles. We can also observe that when pumping just above λ_{ZD} (spectrum at λ_{P}=1554 nm in Fig.10 (a)) non-solitonic radiation is clearly visible but it does not present any maximum. We believe this is due to the interference between solitons and the DWs which gives rise to the generation of new components at frequencies between the solitons and the dispersive waves, as it was already observed in [31]. When powers higher than 2W are injected into the fiber, the same value of ESW can be obtained when pumping over a large spectral region. In Fig. 10 (b) we can see the output spectra obtained at different pumping wavelengths for an input power of 3W. The behavior changes dramatically. First of all, pump depletion occurs also at longer pumping wavelengths. **Second, flat and square-shaped profiles are obtained also at longer pumping wavelengths. Third, dispersive waves do not present a maximum at any pump wavelength and they appear more attenuated than for lower input powers. This behavior, which can be clearly seen in Fig. 6, is probably due to an increasing influence of Raman scattering. We clearly observed an increasing attenuation of the blue-shifted part of the spectrum with increasing input power above the Raman threshold. This effect must be taken into account because it strongly limits the performances of supercontinua in conventional fibers. In fact, although long propagation lengths allow to compensate for a smaller nonlinearity compared to high nonlinear fibers because the SSFS is proportional to the propagation distance [19], broad and high-power spectra can only be obtained at wavelengths above λ_{ZD}. This dynamics limit the spectral region of**

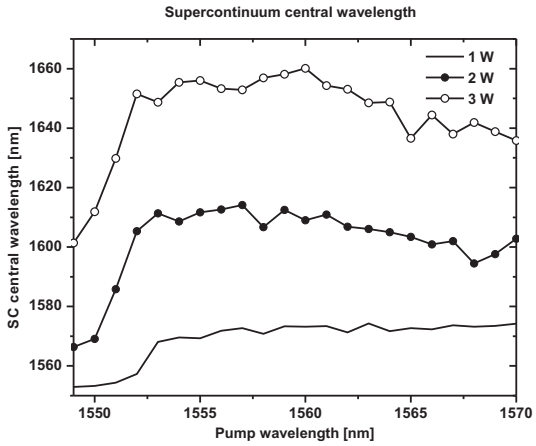

Fig. 12. Supercontinuum central wavelength as function of pump wavelength. Values are shown for input powers of 1W, 2W and 3W

available SC sources in conventional fibers. In order to prove this, we give a rough estimation of the contribution of DWs to the total SC spectrum by calculating the ratio between the spectral power at shorter wavelengths than λ_{ZD} and the total spectral power. It is shown in Fig. 11 for different input powers and wavelengths. It is clear that the contribution of the DWs to spectral broadening is decreasing for increasing input powers and for larger values of dispersion. Dispersive waves tend to disappear with increasing power and an efficient Raman SSFS gives rise to a further red-shifted broad and smooth spectrum. The central wavelength (the average wavelength weighted over the spectral distribution) **for three different input powers** has been plotted in Fig. 12. As it can be seen, it does not change significantly with the input laser wavelength but it is significantly red-shifted with increasing input power.

V. CONCLUSIONS

We have studied experimentally the influence of chromatic dispersion on nonlinear pump spectral broadening and CW-pumped supercontinuum generation in km-long standard fibers. This study has been done by pumping a dispersion shifted fiber with a high-power tunable CW laser source. By sweeping the wavelength of the laser over a small range, we can propagate the pump under very different values of chromatic dispersion but similar values of nonlinear coefficient, attenuation and higher-order dispersive terms. **For a given fiber length**, our results show that, at low input powers, chromatic dispersion plays a dominant role on nonlinear pump spectral broadening, giving rise to a broader spectrum when pumping just above the zero-dispersion wavelength of the fiber. At higher input powers, however, the width of the generated supercontinuum spectrum is mostly due to the Raman effect, hence more independent of the value of the chromatic dispersion coefficient. We also show that, in this case, the optimum pumping wavelengths for supercontinuum generation are not so close to the zero-dispersion wavelength of the fiber as in the previous case. We believe that these ideas will be worthy for the engineering of CW-pumped SC sources.

ACKNOWLEDGMENT

We acknowledge financial support from the Ministerio de Educacion y Ciencia through projects TEC2006-09990-C02-01 and TEC2006-09990-C02-02, the support from CSIC through project MeDIOMURO, the support from the Comunidad Autonoma de Madrid through the projects FUTURSEN S-0505/AMB/000374 and FACTOTEM S-0505/ESP/000417, and the support from Social European Fund through the grant program I3P of CSIC. We acknowledge Prof. Lopez-Higuera from UC for generously lending us his optical filter **and Dr Ania-Castañón from Instituto de Óptica "Daza de valdés" for useful discussions**.

REFERENCES

[1] J. G. Fujimoto, "Optical coherence tomography for ultra high resolution in vivo imaging," *Nat. Biotechnol.*, vol. 21, no. 11, pp. 1361–1367, 2003.

[2] P. L. Hsiung, Y. Chen, T. H. Ko, J. G. Fujimoto, C. J. S. de Matos, S. V. Popov, J. R. Taylor, and V. P. Gapontsev, "Optical coherence tomography using a continuous-wave, high power, raman continuum light source," *Opt. Express*, vol. 12, no. 22, pp. 5287–5295, 2004.

[3] C. J. S. D. Matos, S. V. Popov, and J. R. Taylor, "Temporal and noise characteristics of continuous-wave-pumped continuum generation in holey fibers around 1300 nm," *Appl. Phys. Lett.*, vol. 85, no. 14, pp. 2706–2708, 2004.

[4] S. Martin-Lopez, M. Gonzalez-Herraez, A. Carrasco-Sanz, F. Vanholsbeeck, S. Coen, H. Fernandez, J. Solis, P. Corredera, and M. L. Hernanz, "Broadband spectrally flat and high power density light source for fibre sensing pourposes," *Meas. Sci. Technol.*, vol. 17, no. 5, pp. 1014–1019, 2006.

[5] M. Prabhu, A. Taniguhci, S. Hirose, J. Lu, M. Musha, A. Shirakawa, and K. Ueda, "Supercontinuum generation using raman fiber laser," *Appl. Phys. B-Lasers O.*, vol. 77, no. 2-3, pp. 205–210, 2003.

[6] M. Gonzalez-Herraez, S. Martin-Lopez, P. Corredera, M. L. Hernanz, and P. R. Horche, "Supercontinuum generation using a continuous-wave raman fiber laser," *Opt. Comm.*, vol. 226, no. 1, pp. 323–328, 2003.

[7] P. A. Champert, V. Couderc, and A. Barthelemy, "1.5-2.0 μm multiwatt continuum generation in dispersion-shifted fiber by use of high-power continuous-wave fiber source," *IEEE Photonic. Tech. L.*, vol. 16, no. 11, pp. 2445–2447, 2004.

[8] A. K. Abeeluck, C. Headley, and C. G. Jorgensen, "High-power supercontinuum generation in highly nonlinear, dispersion-shifted fibers by use of a continuous-wave raman fiber laser," *Opt. Lett.*, vol. 29, no. 18, pp. 2163–2165, 2004.

[9] T. Sylvestre, A. Vedadi, H. Maillotte, F. Vanholsbeeck, and S. Coen, "Supercontinuum generation using continuous-wave multiwavelength pumping and dispersion management," *Opt. Lett.*, vol. 31, no. 13, pp. 2036–2038, 2006.

[10] L. Abrardi, S. Martin-Lopez, A. Carrasco-Sanz, P. Corredera, M. L. Hernanz, and M. Gonzalez-Herraez, "Optimized all-fiber supercontinuum source at 1.3 μm generated in a stepwise dispersion-decreasing-fiber arrangement," *IEEE Photonic. Tech. L.*, vol. 25, no. 8, pp. 2098–2012, 2007.

[11] A. Mussot, E. Lantz, H. Maillotte, T. Sylvestre, C. Finot, and S. Pitois, "Spectral broadening of a partially coherent cw laser beam in single-mode optical fibers," *Opt. Express*, vol. 12, no. 13, pp. 2838–2843, 2004.

[12] F. Vanholsbeeck, S. Martin-Lopez, M. Gonzalez-Herraez, and S. Coen, "The role of pump incoherence in continuous-wave supercontinuum generation," *Opt. Express*, vol. 13, no. 17, pp. 6615–6625, 2005.

[13] S. M. Kobtsev and S. V. Smirnov, "Modelling of high-power supercontinuum generation in highly nonlinear dispersion shifted fibers at cw pump," *Opt. Express*, vol. 13, no. 18, pp. 6912–6918, 2005.

[14] M. H. Frosz, O. Bang, and A. Bjarklev, "Soliton collision and raman gain regimes in continuous-wave pumped supercontinuum generation," *Opt. Express*, vol. 14, no. 20, pp. 9391–9407, 2006.

[15] M. N. Islam, G. Sucha, I. Bar-Joseph, M. Wegener, J. P. Gordon, and D. S. Chemla, "Femtosecond distributed soliton spectrum in fibers," *J. Opt. Soc. Am. B*, vol. 6, no. 6, pp. 1149–1158, 1989.

[16] S. Martin-Lopez, M. Gonzalez-Herraez, P. Corredera, M. L. Hernanz, and A. Carrasco, "Experimental investigation of the effect of pump incoherence on nonlinear pump spectral broadening and continuous-wave supercontinuum generation," *Opt. Lett.*, vol. 31, no. 23, pp. 3477–3479, 2006.

[17] A. Hasegawa, "Generation of a train of soliton pulses by induced modulation instability in optical fibers," *Opt. Lett.*, vol. 9, no. 7, pp. 288–290, 1984.

[18] F. M. Mitschke and L. F. Mollenauer, "Discovery of the soliton self-frequency shift," *Opt. Lett.*, vol. 11, no. 10, pp. 659–661, 1986.

[19] J. P. Gordon, "Theory of soliton self-frequency shift," *Opt. Lett.*, vol. 11, no. 10, pp. 662–664, 1986.

[20] J. N. Kutz, C. Lynga, and B. J. Eggleton, "Enhanced supercontinuum generation through dispersion-management," *Opt. Express*, vol. 13, no. 11, pp. 3989–3998, 2005.

[21] B. Costa, D. Mazzoni, M. Puleo, and E. Vezzoni, "Phase-shift technique for measurement of chromatic dispersion in optical fibers using leds," *IEEE J. Quantum Elec.*, vol. 18, no. 10, pp. 1509–1515, 1982.

[22] M. Artiglia, E. Ciaramella, and B. Sordo, "Using modulation instability to determine kerr coefficient in optical fibers," *Electron. Lett.*, vol. 31, no. 12, pp. 1012–1013, 1995.

[23] C. Mazzali, D. F. Grosz, and H. L. Fragnito, "Simple method for measuring dispersion and nonlinear coefficient near the zero-dispersion wavelength of optical fibers," *IEEE Photonic. Tech. L.*, vol. 11, no. 2, pp. 251–253, 1999.

[24] J. Fatome, S. Pitois, and G. Millot, "Measurement of nonlinear and chromatic dispersion parameters of optical fibers using modulation instability," *Opt. Fiber Technol.*, vol. 12, no. 3, pp. 243–250, 2006.

[25] A. Carrasco-Sanz, F. Rodriguez-Barrios, P. Corredera, S. Martin-Lopez, M. Gonzalez-Herraez, and M. L. Hernanz, "An integrating sphere radiometer as a solution for high power calibrations in fiber optics," *Metrologia*, vol. 43, no. 2, pp. 145–150, 2006.

[26] N. Akhmediev and M. Karlsson, "Cherenkov radiation emitted by solitons in optical fibers," *Phys. Rev. A*, vol. 51, no. 3, pp. 2602–2607, 1995.

[27] G. P. Agrawal, *Nonlinear Fiber Optics*. Academic Press, 2001.

[28] K. Tai, A. Tomita, J. L. Jewell, and A. Hasegawa, "Generation of subpicosecond solitonlike optical pulses at 0.3 thz repetition rate by induced modulation instability," *Appl. Phys. Lett.*, vol. 49, no. 5, pp. 236–238, 1986.

[29] Y. Kodama and A. Hasegawa, "Nonlinear pulse propagation in a monomode dielectric guide," *IEEE J. Quantum Elect.*, vol. 23, no. 5, pp. 510–524, 1987.

[30] A. V. Husakou and J. Hermann, "Supercontinuum generation, four-wave mixing, and fission of higher-order solitons in photonic crystal fibers," *J. Opt. Soc. Am. B*, vol. 19, no. 9, pp. 2171–2182, 2002.

[31] J. Hermann, U. Griebner, N. Zhavoronkov, A. Husakou, D. Nickel, J. C. Knight, W. J. Wadsworth, P. S. J. Russel, and G. Korn, "Experimental evidence for supercontinuum generation by fission of higher-order solitons in photonic fibers," *Phys. Rev. Lett.*, vol. 88, no. 17, pp. 173 901.1–173 901.4, 2002.

[32] G. Genty, M. Lehtonen, and H. L. M. Kaivola, "Enhanced bandwidth of supercontinuum generated in microstructured fibers," *Opt. Express*, vol. 12, no. 15, pp. 3471–3480, 2004.

[33] M. H. Frosz, P. Falk, and O. Bang, "The role of the second zero-dispersion wavelength in generation of supercontinua and bright-bright soliton-pairs across the zero-dispersion wavelength," *Opt. Express*, vol. 13, no. 16, pp. 6181–6192, 2005.

[34] J. M. Dudley, G. Genty, and S. Coen, "Supercontinuum generation in photonic crystal fiber," *Rev. Mod. Phys.*, vol. 78, no. 4, pp. 1135–1184, 2006.

[35] I. Cristiani, R. Tediosi, L. Tartara, and V. Degiorgio, "Dispersive waves generation by solitons in microstructured optical fibers," *Opt. Express*, vol. 12, no. 1, pp. 124–135, 2004.

[36] P. K. A. Wai, H. H. Chen, and Y. C. Lee, "Radiation by "solitons" at the zero group-dispersion wavelength of single-mode optical fibers," *Phys. Rev. Lett.*, vol. 41, no. 1, pp. 426–439, 1990.

[37] R. Stolen and E. Ippen, "Raman gain in glass optical waveguides," *Appl. Phys. Lett.*, vol. 22, no. 6, pp. 276–278, 1973.

[38] E. A. Golovchenko, P. V. Mamyshev, A. N. Pilipetskii, and E. M. Dianov, "Numerical analysis of the raman spectrum evolution and soliton pulse generation in single-mode fibers," *J. Opt. Soc. Am. B*, vol. 8, no. 8, pp. 1626–1632, 1991.

[39] D. R. Solli, C. Ropers, P. Koonath, and B. jalali, "Optical rogue waves," *Nature*, vol. 450, no. 13, pp. 1054–1057, 2008.

[40] J. M. Dudley, G. Genty, and B. J. Eggleton, "Harnessing and control of optical rogue waves in supercontinuum generation," *Opt. Express*, vol. 16, no. 6, pp. 3644–3651, 2008.

[41] R. Trebino, *Frequency-resolved optical gating: the measurement of ultrashort laser pulses*. Kluwer Academic Publisher, 2002.